0022-3565/06/3193-1376–1385$20.00
THE JOURNAL OF PHARMACOLOGY AND EXPERIMENTAL THERAPEUTICS
Vol. 319, No. 3
111559/3155491
Printed in U.S.A.

JPET 319:1376–1385, 2006

A-740003 [*N*-(1-{[(Cyanoimino)(5-quinolinylamino) methyl]amino}-2,2-dimethylpropyl)-2-(3,4-dimethoxyphenyl)acetamide], a Novel and Selective $P2X_7$ Receptor Antagonist, Dose-Dependently Reduces Neuropathic Pain in the Rat

Prisca Honore,[1] Diana Donnelly-Roberts,[1] Marian T. Namovic, Gin Hsieh, Chang Z. Zhu, Joe P. Mikusa, Gricelda Hernandez, Chengmin Zhong, Donna M. Gauvin, Prasant Chandran, Richard Harris, Arturo Perez Medrano, William Carroll, Kennan Marsh, James P. Sullivan, Connie R. Faltynek, and Michael F. Jarvis

Neuroscience Research, Global Pharmaceutical Research and Development, Abbott Laboratories, Abbott Park, Illinois

Received July 26, 2006; accepted September 14, 2006

ABSTRACT

ATP-sensitive $P2X_7$ receptors are localized on cells of immunological origin including glial cells in the central nervous system. Activation of $P2X_7$ receptors leads to rapid changes in intracellular calcium concentrations, release of the proinflammatory cytokine interleukin-1β (IL-1β), and following prolonged agonist exposure, cytolytic plasma membrane pore formation. $P2X_7$ knockout mice show reduced inflammation as well as decreased nociceptive sensitivity following peripheral nerve injury. A-740003 (*N*-(1-{[(cyanoimino)(5-quinolinylamino) methyl] amino}-2,2-dimethylpropyl)-2-(3,4-dimethoxyphenyl)acetamide) is a novel competitive antagonist of $P2X_7$ receptors (IC_{50} values = 40 nM for human and 18 nM for rat) as measured by agonist-stimulated changes in intracellular calcium concentrations. A-740003 showed weak or no activity ($IC_{50} > 10$ μM) at other P2 receptors and an array of other neurotransmitter and peptide receptors, ion channels, reuptake sites, and enzymes. A-740003 potently blocked agonist-evoked IL-1β release (IC_{50} = 156 nM) and pore formation (IC_{50} = 92 nM) in differentiated human THP-1 cells. Systemic administration of A-740003 produced dose-dependent antinociception in a spinal nerve ligation model (ED_{50} = 19 mg/kg i.p.) in the rat. A-740003 also attenuated tactile allodynia in two other models of neuropathic pain, chronic constriction injury of the sciatic nerve and vincristine-induced neuropathy. In addition, A-740003 effectively reduced thermal hyperalgesia observed following intraplantar administration of carrageenan or complete Freund's adjuvant (ED_{50} = 38–54 mg/kg i.p.). A-740003 was ineffective in attenuating acute thermal nociception in normal rats and did not alter motor performance at analgesic doses. These data demonstrate that selective blockade of $P2X_7$ receptors in vivo produces significant antinociception in animal models of neuropathic and inflammatory pain.

$P2X_7$ receptors belong to the family of ATP-sensitive ionotropic P2X receptors, which are composed of seven receptor subtypes ($P2X_1$–$P2X_7$) (North, 2002). Unlike other members of the P2 receptor superfamily, homomeric $P2X_7$ receptors are activated by high concentrations of ATP (>100 μM), and 2′,3′-*O*-(4-benzoylbenzoyl)-ATP (BzATP) has significantly greater potency (EC_{50} = 20 μM) than ATP ($EC_{50} > 100$ μM) (Jacobson et al., 2002). $P2X_7$ receptors are found predominantly on macrophages and other cells of immunological origin, where they can trigger a series of cellular responses such as membrane permeabilization, activation of caspases, cytokine release, cell proliferation, and apoptosis (Panenka et al., 2001; Chakfe et al., 2002; North, 2002; Verhoef et al.,

[1] These authors contributed equally to this work.

Article, publication date, and citation information can be found at http://jpet.aspetjournals.org.
doi:10.1124/jpet.106.111559.

ABBREVIATIONS: BzATP, 2′,3′-*O*-(4-benzoylbenzoyl)-ATP; IL, interleukin; A-740003, *N*-(1-{[(cyanoimino)(5-quinolinylamino) methyl]amino}-2,2-dimethylpropyl)-2-(3,4-dimethoxyphenyl)acetamide; PPADS, pyridoxal phosphate-6-azophenyl-2–4-disulfonic acid; KN-62, 1-[*N*,*O*-bis(5-isoquinolinesulfonyl)-*N*-methyl-L-tyrosyl]-4-phenylpiperazine; Yo-Pro, 1(4-[(3-methyl-2(3*H*)-benzoxazolylidene)methyl]-1[3-(trimethylammonio)propyl]-diiodide; DPBS, Dulbecco's phosphate-buffered saline; LPS, lipopolysaccharide; IFN-γ, interferon-γ; PWL, paw-withdrawal latency; CFA, complete Freund's adjuvant; PWT, paw-withdrawal threshold; SNL, spinal nerve ligation; CCI, chronic constriction injury of the sciatic nerve; CNS, central nervous system; TNF, tumor necrosis factor; IL-1ra, IL-1 receptor antagonist; BBG, Brilliant Blue G.

2003; Kahlenberg and Dubyak, 2004). In addition to agonist-induced changes in intracellular calcium concentrations, activation of $P2X_7$ receptors stimulates caspase-1 activation, release of interleukin-1β (IL-1β), and activation of p38 mitogen-activated protein kinase (Armstrong et al., 2002; Ferrari et al., 2006). Another feature of $P2X_7$ receptors is that prolonged agonist exposure leads to the formation of large cytolytic pores in cell membranes (Surprenant et al., 1996). The underlying mechanisms and functional significance of $P2X_7$-mediated pore formation remain to be elucidated; however, $P2X_7$-mediated pore formation is dependent on intracellular signaling events involving, at least in part, p38 mitogen-activated protein kinase and caspase-1 (Pannicke et al., 2000; North, 2002; Donnelly-Roberts et al., 2004).

Both the localization of $P2X_7$ receptors on proinflammatory cells and the demonstration that activation of $P2X_7$ receptors modulates the release of IL-1 have implicated a role for this P2X receptor in inflammatory diseases (North, 2002; Baraldi et al., 2003). A proinflammatory role for $P2X_7$ receptors in inflammation was further supported by the demonstration that $P2X_7$ knockout mice showed reduced inflammation in an experimental passive collagen-induced arthritis model (Labasi et al., 2002). More recently, it was demonstrated that $P2X_7$ knockout mice also show reduced inflammatory thermal hyperalgesia and nerve injury-induced mechanical allodynia as compared with matched wild-type mice (Chessell et al., 2005).

Although the expression of $P2X_7$ receptors has been reported in brain, microglia, and astrocytes based on immunoreactivity studies (Collo et al., 1997; Sim et al., 2004), considerable controversy exists regarding the existence of functional $P2X_7$ receptors on peripheral and central neurons due to the poor specificity of primary antibodies and ligands targeting the rat $P2X_7$ receptor (Anderson and Nedergaard, 2006). However, functional $P2X_7$ receptors have been demonstrated on peripheral glial cells in rat dorsal root ganglion, and this expression may play a role in peripheral sensory transduction of pain perception (Zhang et al., 2005). The present study describes the pharmacological characterization of A-740003 (Fig. 1), a structurally novel and highly specific antagonist for mammalian $P2X_7$ receptors that dose-dependently reduces nociception in rodent models of neuropathic and inflammatory pain.

Materials and Methods

In Vitro Characterization of A-740003

Materials. BzATP, pyridoxal phosphate-6-azophenyl-2–4-disulfonic acid (PPADS), and Brilliant Blue G were purchased from Sigma-Aldrich (St. Louis, MO). KN-62 was purchased from Tocris (Ellisville, MO). Fluo-4 dye was purchased from TEF Labs (Austin TX), and Yo-Pro was purchased from Invitrogen (Eugene, OR). All cell culture medium and Dulbecco's phosphate-buffered saline (DPBS), pH 7.4, were also obtained from Invitrogen (Grand Island, NY).

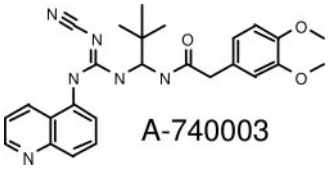

Fig. 1. Structure of A-740003.

Cell Culture. 1321N1 human astrocytoma cells stably expressing human and rat $P2X_7$, human $P2X_4$, $P2X_{2a}$, $P2X_{2/3}$, $P2X_1$, $P2Y_1$, and $P2Y_2$ recombinant receptors were grown according to previously published protocols (Bianchi et al., 1999; Lynch et al., 1999). Briefly, 1321N1 cells expressing transfected P2 receptors were maintained in a humidified 5% CO_2 atmosphere at 37°C in Dulbecco's modified Eagle's medium containing 1% L-alanyl-L-glutamine, 1% antibiotic/antimycotic, 10% fetal bovine serum, and 300 μg/ml geneticin. 1321N1 $P2X_{2a}$ cells were grown in Dulbecco's modified Eagle's medium containing 1% L-alanyl-L-glutamine, 1% antibiotic/antimycotic, 10% fetal bovine serum, and 100 μg/ml hygromycin B. 1321N1 $P2X_{2a/3}$ cells were maintained in growth medium containing 150 μg/ml geneticin and 75 μg/ml hygromycin B. Cells of the THP-1 monocytic cell line (American Type Culture Collection, Rockville, MD) were maintained in the log phase of growth in RPMI 1640 medium containing high glucose and 10% fetal calf serum (Invitrogen) according to established procedures (Humphrey and Dubyak, 1996). Fresh vials of frozen THP-1 cells were initiated for growth every 8 weeks. To differentiate THP-1 cells into a macrophage phenotype, a final concentration of 25 ng/ml LPS and 10 ng/ml IFN-γ were added to the cells (Humphrey and Dubyak, 1996) either for 3 h for IL-1β release assays or overnight (16 h) for pore formation studies.

Ca^{2+} Influx Assay. Agonist-induced changes in intracellular Ca^{2+} concentrations were assessed in all of the cell lines using the Ca^{2+} chelating dye, Fluo-4 in conjunction with a fluorometric imaging plate reader (Molecular Devices, Sunnyvale, CA) as previously described (Bianchi et al., 1999) with minor modifications. The cells were plated out the day before the experiment onto Poly-D-lysine-coated black 96-well plates (Becton-Dickinson, Bedford, MA; Sigma-Aldrich). Cell concentration was 5×10^6 cells per plate. Fluo-4 was dissolved in anhydrous dimethyl sulfoxide to a final concentration of 5 μM in DPBS. The dye was loaded onto the adherent cells, and the plates were centrifuged for 5 min at 1000 rpm. Cells were loaded for at least 1 h but not more than 3 h and kept in the dark at room temperature. After loading, the unincorporated Fluo-4 was removed by washing with DPBS using a SkanWasher 400 (Molecular Devices). All compound solutions were prepared in DPBS. After the agonist addition, changes in intracellular Ca^{2+} concentrations were recorded on a second time scale for 3 min. Ligands were tested at 11 half-log concentrations from 10^{-10} to 10^{-4} M. Independent measurements of a positive control (100%) were performed on each plate to normalize values from plate to plate. Agonist concentrations corresponded to their relative EC_{70} values for each receptor to enable comparison of antagonist potencies across multiple P2 receptor subtypes (Jarvis et al., 2002). Since $P2X_{2/3}$ receptors have an identical pharmacological profile as homomeric $P2X_3$ receptors and do not rapidly desensitize (Jarvis et al., 2004), the heteromeric receptor was used for selectivity versus $P2X_3$ receptors. Structural analogs of A-740003, as well as other structurally diverse $P2X_7$ antagonists (Nelson et al., 2006), did not activate homomeric $P2X_3$ receptors at concentrations up to 10 μM (D. Donnelly-Roberts, unpublished data). For measurement of antagonist activity, ligands were added to the cell plate, and fluorescence data were collected for 3 min before the addition of the agonist. Fluorescence data were collected for another 2 min after the agonist addition. Concentration-response data were analyzed using Prism (GraphPad Software, Inc., San Diego, CA); the pEC_{50} or pIC_{50} values were derived from a single curve fit to the mean data ($n = 4–6$) in duplicate.

Yo-Pro Uptake Assay. Agonist-induced pore formation was assessed using uptake of Yo-Pro dye (mol. wt. = 629; Invitrogen) in the recombinant rat, human $P2X_7$-1321N1 cell lines, or differentiated THP-1 cells as previously described (Donnelly-Roberts et al., 2004). Yo-Pro iodide dye (1 mM in 100% dimethyl sulfoxide) was diluted to a final concentration of 2 μM in PBS (without Mg^{2+} or Ca^{2+}) and then placed on the cells immediately prior to agonist addition. Cells were plated the day before at a density of 1×10^6 cells/ plate onto poly-D-lysine-coated black-walled 96-well plates to reduce light scat-

tering. For differentiated THP-1 (25 ng/ml LPS and 10 ng/ml IFN-γ overnight), the cells were plated onto poly-D-lysine-coated black-walled 96-well plates to 1 to 2 × 10^6 cells/ml/well. After the addition of various concentrations of agonists, the Yo-Pro dye uptake was observed in the fluorometric imaging plate reader by capturing the intensity of fluorescence by the CCD camera every 15 s for the first 10 min of agonist exposure followed by every 20 s for an additional 50 min. For antagonist activity measurements, the percent maximal intensity was normalized to that induced by an EC_{70} concentration for BzATP activation and plotted against the antagonist compound concentration to calculate IC_{50} values and account for plate-to-plate variability. Concentration-response data were analyzed using GraphPad Prism; the pEC_{50} or pIC_{50} values were derived from a single curve fit to the mean data of $n = 6$ in duplicates.

IL-1β Release in THP-1 Cells. In the presence of the differentiation media, THP-1 cells were incubated with inhibitors for 30 min at 37°C followed by a challenge with 1 mM BzATP for an additional 30 min at 37°C. Supernatants were collected after a 5-min centrifugation in microfuge tubes and assayed for the presence of mature IL-1β by enzyme-linked immunosorbent assay (Endogen, Rockford, IL), following the manufacturer's instructions. For each experiment, differentiated control cells were also measured over the 60-min time course of the assay to assess background IL-1β accumulation. This nonspecific background IL-1β release, which typically averaged 38% of the maximal BzATP response, was subtracted from the maximal BzATP-induced release.

In Vivo Pain Models and Pharmacokinetic Profile

Subjects. Male Sprague-Dawley rats (Charles River, Wilmington, MA) weighing 200 to 300 g were used in all experiments. Animals were group-housed in Association for Assessment and Accreditation of Laboratory Animal Care-approved facilities at Abbott Laboratories (Abbott Park, IL) in a temperature-regulated environment with lights on between 7:00 AM and 8:00 PM. Food and water were available ad libitum except during testing. All animal handling and experimental protocols were approved by an institutional animal care and use committee. All experiments were performed during the light cycle.

Acute Thermal Nociception. The response to acute thermal stimulation was determined using a commercially available paw thermal stimulator (UARDG; University of California, San Diego, CA). Rats were placed individually in Plexiglas cubicles mounted on a glass surface maintained at 30°C and allowed a 30-min habituation period. A thermal stimulus, in the form of radiant heat emitted from a focused projection bulb, was then applied to the plantar surface of each hind paw. In each test session, each rat was tested in three sequential trials at approximately 5-min intervals. Paw-withdrawal latencies (PWLs) were calculated as the median of the two shortest latencies. An assay cut off was set at 20.5 s. A-740003 was injected i.p. 30 min before testing for acute thermal pain.

Carrageenan and Complete Freund's Adjuvant-Induced Thermal Hyperalgesia and Edema. Unilateral inflammation was induced by injecting 100 μl of a 1% solution of λ-carrageenan or 150 μl of a 50% solution of complete Freund's adjuvant (CFA) (Sigma-Aldrich) in physiological saline into the plantar surface of the right hind paw of the rat. The hyperalgesia to thermal stimulation was determined 2 or 48 h following carrageenan or CFA injection, respectively, using the same apparatus as described above for the noxious acute thermal assay. In addition, in both models, the volume of paw edema was measured using water displacement with a plethysmometer (Buxco, Sharon, CT) by submerging the hind paw up to the ankle hairline (approximately 1.5 cm). The volume of water displacement was measured by a transducer and recorded by a computer. A-740003 was injected 90 min following carrageenan injection (i.e., 30 min before testing in inflamed rats). In the CFA experiments, CFA was injected 2 days before testing. On the day of testing, A-740003 was injected 30 min i.p. before testing for thermal hyperalgesia.

Spinal Nerve (L_5/L_6) Ligation Model of Neuropathic Pain. As previously described in detail by Kim and Chung (1992), a 1.5-cm incision was made dorsal to the lumbosacral plexus in anesthetized rats. The paraspinal muscles (left side) were separated from the spinous processes, the L_5 and L_6 spinal nerves were isolated, and tightly ligated with 3-0 silk threads. Following hemostasis, the wound was sutured and coated with antibiotic ointment. The rats were allowed to recover and then placed in a cage with soft bedding for 14 days before behavioral testing for mechanical allodynia. A-740003 was injected i.p. 30 min before testing for mechanical allodynia.

Mechanical (tactile) allodynia was measured using calibrated von Frey filaments (Stoelting, Wood Dale, IL). Briefly, rats were placed into individual Plexiglas containers and allowed to acclimate for 15 to 20 min before testing. Paw withdrawal threshold ($PWT_{vonfrey}$) was determined by increasing and decreasing stimulus intensity and estimated using a Dixon nonparametric test. Only rats with threshold scores ≤ 4.5 g were considered allodynic and utilized in compound testing experiments.

Sciatic Nerve Ligation Model of Neuropathic Pain. As previously described in detail by Bennett and Xie (1988), in anesthetized rats, a 1.5-cm incision was made 0.5 cm below the pelvis, and the biceps femoris and the gluteous superficialis (right side) were separated. The sciatic nerve was exposed, isolated, and four loose ligatures (5-0 chromic catgut) with 1-mm spacing were placed around it. The rats were allowed to recover and then placed in a cage with soft bedding for 14 days before behavioral testing for mechanical allodynia as described above. A-740003 was injected i.p. 30 min before testing for mechanical allodynia.

Chemotherapy-Induced Neuropathic Pain. As previously described in detail by Lynch et al. (2005), chemotherapy-induced neuropathic pain was induced by a continuous i.v. infusion of vincristine. In anesthetized rats, the right external jugular vein was catheterized (PE60 tubing) with a vincristine filled osmotic pump (0.5 μl/h, 14 days; Alzet model 2002; Durect Corporation, Cupertino, CA) that had been primed overnight to deliver 30 μg/kg/day vincristine sulfate (Sigma-Aldrich). The rats were allowed to recover and then placed in a cage with soft bedding for 14 days before behavioral testing for mechanical allodynia as described above. A-740003 was injected i.p. 30 min before testing for mechanical allodynia. In this model, because of the bilateral allodynia, maximal possible effects were set at 15 g.

Rotorod Performance. Rotorod performance was measured using an accelerating Rotorod apparatus (Omnitech Electronics, Inc., Columbus, OH). Rats were allowed a 30-min acclimation period in the testing room and then placed on a 9-cm-diameter rod that increased in speed from 0 to 20 rpm over a 60-s period. The time required for the rat to fall from the rod was recorded, with a maximal score of 60 s. Each rat was given three training sessions. Rotorod performance (latencies to fall from the Rotorod) was determined 30 min following i.p. A-740003 injection.

Compounds. A-740003 (Fig. 1) was synthesized at Abbott Laboratories. A-740003 was dissolved in 30% *N*-methylpyrrolidinone, 30% polyethylene glycol, and 40% hydroxypropyl-β-cyclodextrin for i.p. administration 30 min before testing and in 100% polyethylene glycol for p.o. administration 60 min before testing in a 2-ml/kg dosing volume. As part of an ongoing drug discovery program, doses of A-740003 ranged from 10 to 300 μmol/kg for relative comparisons of compound potency. Doses of A-74003 used in the in vivo studies are expressed as milligrams per kilogram in this report for clarity.

Statistics. Analysis of the in vivo data were carried out using analysis of variance. Where appropriate, Fisher's protected least significant difference was used for post hoc analysis. The level of significance was set at $p < 0.05$. ED_{50} values were estimated using least squares linear regression. Data are presented as mean ± S.E.M.

Results

A-740003 Potently Blocks $P2X_7$ Receptors. A-740003 potently blocked BzATP-evoked changes in intracellular calcium concentrations in 1321N1 cells stably expressing rat (IC_{50} = 18 nM) or human (IC_{50} = 40 nM) $P2X_7$ receptors (Fig. 2). For comparison, PPADS, Brilliant Blue G (rat selective $P2X_7$ antagonist), and KN-62 (a human selective $P2X_7$ antagonist; Anderson and Nedergaard, 2006) were significantly less potent in blocking BzATP-evoked changes in intracellular calcium concentrations (Fig. 2; Table 1). A-740003 also blocked BzATP-mediated pore formation as measured by the intracellular uptake of Yo-Pro (Fig. 3) at both the rat (IC_{50} = 138 nM) and human (IC_{50} = 93 nM) $P2X_7$ receptors. A-740003 was significantly more potent in blocking $P2X_7$-mediated pore formation as compared with PPADS, KN-62, or Brilliant Blue G (Table 1; Fig. 3).

A-740003 Blocks $P2X_7$ Receptors on Differentiated Human THP-1 Cells. Human THP-1 cells differentiated with LPS and IFN-γ into a macrophage phenotype express $P2X_7$ receptors and receptor activation lead to IL-1β release as well as Yo-Pro uptake (Humphrey and Dubyak, 1996; Donnelly-Roberts et al., 2004). A-740003 potently blocked Yo-Pro uptake in differentiated human THP-1 cells (IC_{50} of 92 nM) (Fig. 4). A-740003 also blocked IL-1β release in the THP-1 cells (IC_{50} of 156 nM) (Fig. 4).

A-740003 Is a Highly Selective $P2X_7$ Antagonist. As shown in Fig. 5, A-740003, at concentrations up to 100 μM, did not significantly reduce agonist-evoked changes in intracellular calcium concentrations mediated by a variety of other P2X and P2Y receptors. We have demonstrated previously that there is a high positive correlation (r = 0.98) between ligand binding at heteromeric $P2X_{2/3}$ receptors and homomeric $P2X_3$ receptors (Jarvis et al., 2004). Consequently, A-740003 was not tested at homomeric $P2X_3$ receptors since it was inactive at $P2X_{2/3}$ receptors. Other analogs of A-740003, as well as other structurally novel $P2X_7$ receptor antagonists (Nelson et al., 2006), did not significantly interact at homomeric $P2X_3$ receptors at concentrations up to 10 μM (D. Donnelly-Roberts, unpublished data). A-740003 was also evaluated for its ability to interact with a large array of

TABLE 1
Functional pharmacological evaluation
pIC_{50} values represent means determined from at least three separate experiments.

Antagonist	Rat $P2X_7$	Human $P2X_7$
$[Ca^{2+}]_I$ (pIC_{50} ± S.E.M.)		
A-740003	7.75 ± 0.03	7.36 ± 0.04
PPADS	5.10 ± 0.02	5.45 ± 0.03
KN62	<4	4.88 ± 0.18
BBG	5.08 ± 0.07	<4
Yo-Pro Activity (pIC_{50} ± S.E.M.)		
A-740003	7.00 ± 0.02	7.03 ± 0.04
PPADS	5.92 ± 0.09	5.88 ± 0.03
KN62	<4	6.67 ± 0.02
BBG	6.22 ± 0.03	5.71 ± 0.09

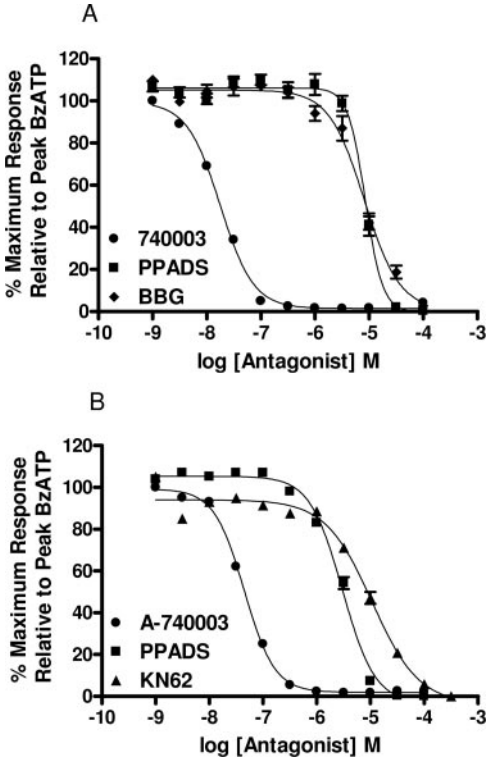

Fig. 2. A-740003 potently blocks rat and human $P2X_7$ receptors. A-740003 blocked BzATP-mediated changes in intracellular calcium concentrations at rat (10 μM BzATP) (A) and human (5 μM BzATP) (B) $P2X_7$ receptors. PPADS and BBG were significantly less potent, and KN-62 showed no activity (Table 1) to block rat $P2X_7$ receptors. Similarly, PPADS and KN-62 were significantly less potent, and BBG showed no activity (Table 1) to block human $P2X_7$ receptors. Data are represented in percentage of maximal response (control) minus basal fluorescence. See Table 1 for a summary of the pIC_{50} values.

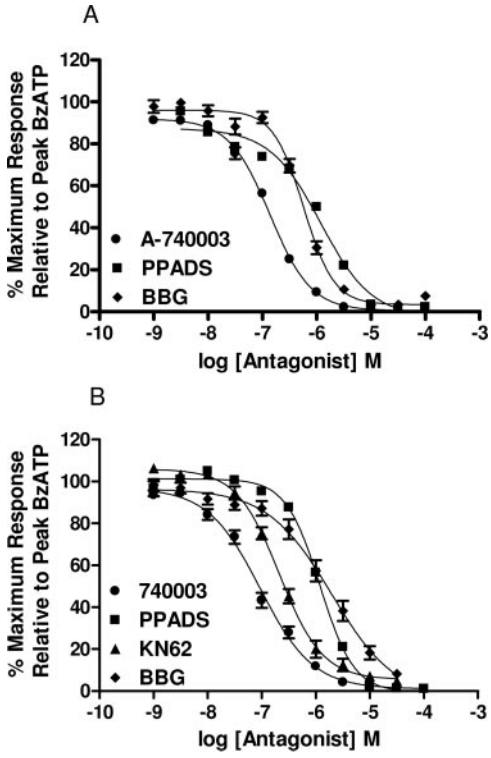

Fig. 3. A-740003 potently blocks pore formation mediated by rat and human $P2X_7$ receptors. A-740003 blocked BzATP-mediated Yo-Pro uptake at rat (7.5 μM BzATP) (A) and human (2.5 μM BzATP) (B) $P2X_7$ receptors. PPADS and BBG were significantly less potent, and KN-62 showed negligible activity (Table 1) to block rat $P2X_7$ receptors. Similarly, KN-62 was slightly less potent versus PPADS and BBG, which had weaker activity (Table 1) to block human $P2X_7$ receptors. Data are represented in percentage of maximal response (control) minus basal fluorescence. See Table 1 for a summary of the pIC_{50} values.

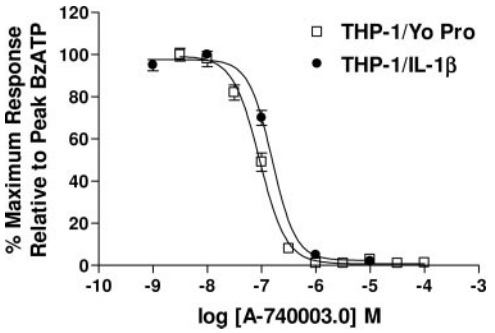

Fig. 4. A-740003 potently blocks native human $P2X_7$ receptors expressed in differentiated THP-1 cells. A-740003 blocked 90 μM BzATP-mediated changes in both pore formation (□) or IL-1β release (●) in differentiated human THP-1 by addition of the antagonist 30 min before agonist stimulation with BzATP, as described under *Materials and Methods*. Data are represented as percentage of maximal response (control) minus basal fluorescence.

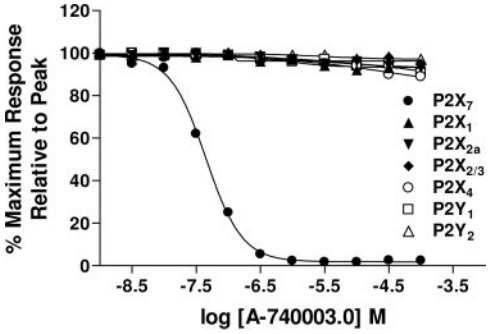

Fig. 5. A-740003 is a highly selective $P2X_7$ antagonist. A-740003 selectively blocks $P2X_7$ receptors and not other P2 subtypes. ATP (4 μM) was used to activate $P2X_1$, $P2X_4$, and $P2Y_1$ receptors, and ATP (10 μM) was used for $P2X_{2a}$ and $P2X_{2a/3}$ receptors. UTP (1 μM) was used to activate $P2Y_2$ receptors. BzATP (5 μM) was used for human $P2X_7$ receptors. Data are represented in percentage of maximal response (control) minus basal fluorescence.

G-protein-coupled receptors, enzymes, transporters, and ion channels (CEREP, Poitiers, France; http://www.cerep.fr/cerep/users/pages/catalog/assay/catalog.asp) (Table 2). A-740003 showed weak or no activity in all of these assays ($IC_{50} > 5$ μM).

A-740003 Is a Competitive Antagonist at the $P2X_7$ Receptor. To determine the nature of the antagonism of $P2X_7$ receptors by A-740003, BzATP concentration-effect curves were determined in the presence of increasing concentrations of A-740003. Figure 6 shows that BzATP concentration-effect curves were shifted to the right with increasing A-740003 concentrations, without affecting the maximal BzATP response in control wells. These results indicated that A-740003 acts as a competitive antagonist at the $P2X_7R$ BzATP binding site. Analysis of these data generated a pA_2 value of 7.30 and a slope factor of 0.98 ± 0.16 (Fig. 6).

Pharmacokinetic Profile of A-740003. The pharmacokinetic profile of A-740003 in rats (Fig. 7) was characterized by high plasma clearance (3.7 l/h/kg), moderate oral bioavailability (F = 20%), a high volume of distribution (V_β = 21 l/kg), and a long plasma elimination half-life ($t_{1/2}$ = 4.0 h i.v.). The maximal plasma concentration (C_{max}) and time to maximal plasma concentration (T_{max}) following oral administration at 2 mg/kg were 0.13 μg/ml and 2.5 h, respectively. In addition, A-740003 had good bioavailability (F = 79%) following i.p. administration at 2 mg/kg with a C_{max} of 0.76 μg/ml and a T_{max} of 0.25 h. Plasma and spinal cord samples were harvested 30 min following i.p. administration. Mean plasma levels of A-740003 were 5.5 ± 1.2 μg/ml at 14.2 mg/kg and 18.4 ± 4.6 μg/ml at 47.4 mg/kg, and brain levels were 0.6 ± 0.2 μg/g at 14.2 mg/kg and 1.0 ± 0.3 μg/g at 47.4 mg/kg.

Spinal Nerve Injury-Induced Mechanical Allodynia. L_5-L_6 spinal nerve ligation (SNL; Kim and Chung, 1992) induced a decrease in $PWT_{vonfrey}$ to mechanical stimulation with von Frey monofilaments 2 weeks following injury ($PWT_{vonfrey}$ control, 12.9 ± 0.4 g; $PWT_{vonfrey}$ injured, 2.9 ± 0.1 g; $p < 0.01$), demonstrating the development of mechanical allodynia. A-740003 reversed SNL-induced mechanical allodynia in a dose-related manner (ED_{50} of 19 mg/kg i.p.) with 64.9 ± 11.1% effect at the highest dose tested (Fig. 8; Table 3). In addition, in another set of allodynic SNL animals ($PWT_{vonfrey}$ control, 13.2 ± 0.4 g; $PWT_{vonfrey}$ injured, 3.7 ± 0.1 g; $p < 0.01$), A-740003 reduced SNL-induced mechanical allodynia following oral administration with 37.1 ± 9.5% increase in PWT at 142.4 mg/kg p.o. ($PWT_{vonfrey}$, 7.8 ± 0.9 g; $p < 0.01$ versus vehicle-treated animals, $PWT_{vonfrey}$ injured, 4.3 ± 0.4 g).

Sciatic Nerve Injury-Induced Mechanical Allodynia. Chronic constriction injury of the sciatic nerve (CCI; Bennett and Xie, 1988) produced a decrease in $PWT_{vonfrey}$ to mechanical stimulation with von Frey monofilaments 2 weeks following surgery ($PWT_{vonfrey}$ control, 13.3 ± 0.3 g; $PWT_{vonfrey}$ injured, 2.9 ± 0.1 g; $p < 0.01$), demonstrating the development of mechanical allodynia. A-740003 attenuated CCI-induced mechanical allodynia in a dose-related manner with an ED_{50} of 114 mg/kg i.p. and efficacy of 54.7 ± 14.3% at the highest dose tested (Fig. 9A; Table 3).

Chemotherapy-Induced Mechanical Allodynia. Continuous vincristine infusion produced a decrease in $PWT_{vonfrey}$ to mechanical stimulation with von Frey monofilaments 2 weeks following the beginning of the infusion ($PWT_{vonfrey}$ control, 15.0 ± 0.0 g; $PWT_{vonfrey}$ injured, 3.7 ± 0.1 g; $p < 0.01$), demonstrating the development of mechanical allodynia. A-740003 attenuated vincristine-induced mechanical allodynia in a dose-related manner with 50.8 ± 6.4% effect at the highest dose tested (Fig. 9B; Table 3).

Carrageenan-Induced Acute Inflammatory Thermal Hyperalgesia and Edema. Carrageenan injection into the hind paw induced a significant decrease in PWL to thermal stimulation (PWL control, 9.9 ± 0.2 s versus PWL inflamed, 2.3 ± 0.1 s; $p < 0.01$), demonstrating the development of thermal hyperalgesia 2 h following carrageenan injection (Fig. 10A). A-740003 reduced carrageenan-induced thermal hyperalgesia in a dose-related manner (ED_{50} of 54 mg/kg i.p.), with 75 ± 5% antinociceptive effect at the highest dose tested (Fig. 8A). Under the same conditions, A-740003 had no effect on PWL of the contralateral noninflamed paw, indicative of a specific antihyperalgesic effect in this model.

The acute anti-inflammatory effects of A-740003 were assessed in the carrageenan-induced paw edema model. A-740003 (14–142 mg/kg i.p.) attenuated carrageenan-induced paw edema [$F(3,47) = 4.75$, $p < 0.01$]. At 142 mg/kg i.p., A-740003 produced a 36 ± 7% decrease in paw volume ($p < 0.01$, Table 3).

CFA-Induced Chronic Inflammatory Thermal Hyperalgesia and Edema. CFA injection into the hind paw

TABLE 2
Pharmacological selectivity of A-740003
All assays were conducted at CEREP (http://www.cerep.fr/cerep/users/pages/catalog/assay/catalog.asp) using previously published methods (CEREP, Poitiers, France).

Target	Ligand	~IC_{50}	Target	Ligand	~IC_{50}
		μM			μM
Adenosine A_1	[^{3}H]DPCPX	>10	Angiotensin (AT_1)	[^{125}I][Sar^1,Ile^8]-ATII	>10
Adenosine A_{2A}	[^{3}H]CGS 21680	>10	Angiotensin (AT_2)	[^{125}I]CGP 42112A	>10
Adenosine A_3	[^{125}I]AB-MECA	>10	Bombesin	[^{125}I][Tyr^4]bombensin	>10
Adrenergic α_1	[^{3}H]Prazosin	>10	Bradykinin B2	[^{3}H]NPC 17731	>10
Adrenergic α_2	[^{3}H]RX 821002	>10	CCKA	[^{3}H]Devazepide	>10
Adrenergic β_1	[^{3}H](−)CGP-12177	>10	CCKB	[^{3}H]CCK-8	>10
Adrenergic β_2	[^{3}H](−)CGP-12177	>10	Endothelin (ET_A)	[^{125}I]Endothelin-1	>10
ANP	[^{125}I]ANP	>10	Endothelin (ET_B)	[^{125}I]Endothelin-1	>10
Cannabinoid CB_1	[^{3}H]Win 55212-2	>10	Galanin (GAL1)	[^{125}I]Galanin	>10
Cannabinoid CB_2	[^{3}H]Win 55212-2	>10	PDGF	[^{125}I]PDGF BB	>10
Dopamine D1	[^{3}H]SCH23390	>10	Melatonin (ML1)	[^{125}I]Iodomelatonin	>10
Dopamine D2	[^{3}H]Spiperone	>10	Neurokinin (NK_1)	[^{125}I][Sar^9,Met(O_2)^{11}]-S	>10
Dopamine D3	[^{3}H]Spiperone	>10	Neurokinin (NK_2)	[^{125}I]NKA	>10
Dopamine D4.4	[^{3}H]Spiperone	>10	Neurokinin (NK_3)	[^{125}I][MePhe^7]-NKB	>10
Dopamine D5	[^{3}H]SCH23390	>10	Neuropeptide Y1	[^{125}I]peptide YY	>10
GABA	[^{3}H]GABA	>10	Neuropeptide Y2	[^{125}I]peptide YY	>10
IL-8B (CXCR2)	[^{125}I]IL-8	>10	Neurotensin (NT1)	[^{125}I]Neurotensin	>10
TNFα	[^{125}I]TNFα	>10	Somatostatin	[^{125}I]Tyr^{11}-somatostatin	>10
CCR1	[^{125}I]MIP-1α	>10	VIP_1 ($VPAC_1$)	[^{125}I]VIP	>10
Histamine H1	[^{3}H]Pyrilamine	>10	Vasopressin V1a	[^{3}H]AVP	>10
Histamine H2	[^{125}I]APT	>10	NE transporter	[^{3}H]Nisoxetine	>10
Muscarinic M1	[^{3}H]Pirenzepine	>10	DA uptake	[^{3}H]GBR12935	>10
Muscarinic M2	[^{3}H]AF-DX384	>10	Benzodiazepine central	[^{3}H]Flunitrazepam	>10
Muscarinic M3	[^{3}H]4-DAMP	>10	Benzodiazepine peripheral	[^{3}H]PK11195	5
Muscarinic M4	[^{3}H]4-DAMP	>10	AMPA	[^{3}H]AMPA	>10
Muscarinic M5	[^{3}H]4-DAMP	>10	Kainate	[^{3}H]Kainic acid	>10
Opioid δ2	[^{3}H]DADLE	>10	NMDA	[^{3}H]CGP 39653	>10
Opioid κ	[^{3}H]U-69593	>10	Ca^{2+} channel DHP site	[^{3}H]PN200-110	>10
Opioid μ	[^{3}H]DAMGO	>10	Ca^{2+} channel diltiazem site	[^{3}H]Diltiazem	>10
ORL1	[^{3}H]Nociceptin	>10	Ca^{2+} channel verapamil site	[^{3}H]D 888	>10
PACAP PAC_1	[^{3}H]$PACAP_{1-27}$	>10	Ca^{2+} channel N	[^{125}I]ω-Conotoxin	>10
P2X	[^{3}H]α,βMeATP	>10	K^+ channel (voltage dependent)	[^{125}I]Dendrotoxin	>10
P2Y	[^{35}S]dATPαS	>10	K^+ channel (Ca^{2+} dependent)	[^{125}I]Apmin	>10
Serotonin 5-HT_{1A}	[^{3}H]8-OH-PAT	>10	Na^+ channel (site 2)	[^{3}H]Batrachotoxinin	>10
Serotonin 5-HT_{1B}	[^{3}H]CYP	>10	Cl^- ionophore	[^{35}S]TBPS]	>10
Serotonin 5-HT_{2A}	[^{3}H]Ketanserin	>10	Glycine (strychnine sensitive)	[^{3}H]Strychnine	>10
Serotonin 5-HT_{2C}	[^{3}H]Mesulergine	>10	Glycine (strychnine insensitive)	[^{3}H]MDL105,519	>10
Serotonin 5-HT_3	[^{3}H]BRL 43694	>10	MAO-A	[^{3}H]Ro41-1049	>10
Serotonin 5-HT_{5A}	[^{3}H]LSD	>10	MAO-B	[^{3}H]Ro-19-6327	>10
Serotonin 5-HT_6	[^{3}H]LSD	>10	σ	[^{3}H]DTG	>10
Serotonin 5-HT_7	[^{3}H]LSD	>10	σ_2	[^{3}H]DTG	>10
σ_1	[^{3}H]Pentazocine	>10			

ANP, atrial natriuretic peptide; PACAP, pituitary adenylyl cyclase-activating protein; DPCPX, 8-cyclopentyl-1,3-dipropylxanthine; CGS 21680, 2-[*p*-(2-carboxyethyl)phenethylamino]-5′-*N*-ethylcarboxamidoadenosine; AB-MECA, 4-aminobenzyl-5′-*N*-methylcarboxamidoadenosine; RX 821002, 2-(2-methoxy-1,4-benzodioxan-2yl)-2-imidazoline; CGP-12177, 4-[3-[(1,1-dimethylethyl)amino]-2-hydroxypropoxy]-1,3-dihydro-2*H*-benzimidazol-2-one; SCH23390, *R*-(+)-7-chloro-8-hydroxy-3-methyl-1-phenyl-2,3,4,5-tetrahydro-1*H*-3-benzazepine; 4-DAMP, 4-diphenylacetoxy-*N*-methylpiperidine; DADLE, [D-Ala^2,D-Leu^5]-enkephalin; U-69593, (+)-(5α ,7α ,8β) -*N*-methyl-*N*-[7-(1-pyrrolidinyl)-1-oxaspiro[4.5]dec-8-yl]benzeneacetamide; DAMGO, [D-Ala^2,*N*-Me-Phe^4,Gly^5-ol]-enkephalin; MeATP, methylene-ATP; 8-OH-DPAT, 8-hydroxy-2-dipropylaminotetralin; CYP, cyanopindolol; LSD, *d*-lysergic acid diethylamide; CCK, cholecystokinin; PDGF, platelet-derived growth factor; NE, norepinephrine; DA, dopamine; AMPA, α -amino-3-hydroxy-5-methyl-4-isoxazolepropionic acid; NMDA, *N*-methyl-D-aspartate; DHP, dihydropyridine; MAO, monoamine oxidase; VIP, vasoactive intestinal peptide; AVP, arginine vasopressin; GBR12935, (1-[2-(diphenylmethoxy)ethyl]-4-(3-phenylpropyl)-piperazine); PK11195, 1-(2-chloro-phenyl)-*N*-methyl-*N*-(1-methylpropyl)-1-isoquinoline carboxamide; TBPS, *t*-butylbicyclophosphorothionate; CCR, chemokine receptor; ORL, opioid receptor-like; MIP, macrophage inflammatory protein; APT, aminopotentidine; VPAC, (vasoactive intestinal peptide) pituitary adenylate cyclase-activating peptide receptor; DTG, 1,3-di-*o*-tolyguanidine; WIN 55212-2, (*R*)-(+)-[2,3-dihydro-5-methyl-3-(4-morpholinylmethyl) pyrrolo-[1,2,3-*d*,*e*]-1,4-benzoxazin-6-yl]-1-naphthalenyl-methanone; AF DX384, 5,11-dihydro-11-[2-(-[8-dipropylamino)methyl]-1-piperidinyl]-ethyl]amino]-carbonyl-6*H*-pyrido[2,3-*b*] [1,4]benzodiazepin-6-one; BRL 43694, granisetron; MDL 105,519, (*E*)-3-(2-phenyl-2-carboxylethenyl)-4,6-dichloro-1[^{3}H]-indole-2-carboxylic acid; NPC 17731, D-Arg[Hyp^3,D-HypE-(*transprolyl*)^7,Oic^8]bradykinin; Ro41-1049, *N*-(2-aminoethyl)-5-(*m*-fluorophenyl)-4-thiazole carboxamide HCl; CGP 39653, D,L-(*E*)-2-amino-4-propyl-5-phosphono-3-pentenoic acid; CGP 42112A, *N*-α-nicotinoyl-Tyr-(*N*-α-CBZ-Arg)-Lys-His-Pro-Ile-OH; D 888, verampil derivative; PN200-110, (+)-[^{3}H]isopropyl-4-(2,1,3-benzoxadiazol-4-yl)-1,4-dihydro-5-methoxycarbonyl-2,6-dimethyl-3-pyridinecarboxylate; Ro 19-6327, lazabemide..

induced a significant decrease in PWL to thermal stimulation 48 h following CFA injection (PWL control, 10.2 ± 0.3 s versus PWL inflamed, 5.6 ± 0.1 s, $p < 0.01$), demonstrating the development of thermal hyperalgesia (Fig. 10B). A-740003 attenuated CFA-induced thermal hyperalgesia in a dose-related manner (ED_{50} of 38 mg/kg i.p.) with 58.7 ± 16.5% effect at the highest dose tested (Fig. 10B). Under the same conditions, A-740003 had no effect on PWL of the contralateral noninflamed paw, indicative of a specific antihyperalgesic effect in this model.

The acute anti-inflammatory effects of A-740003 were also assessed in the CFA-induced paw edema model. A-740003 (14–142 mg/kg i.p.) did not significantly decrease CFA-induced paw edema [$F(3,35) = 2.28$, $p > 0.05$; Table 3].

Acute Thermal Pain. A-740003 did not produce significant antinociception on acute thermal pain in naive rats. A-740003 (142 mg/kg i.p.)-treated animals had a PWL to acute thermal stimulation of 10.9 ± 0.1 compared with 10.9 ± 0.5 s in vehicle-treated animals ($p > 0.05$; Table 3).

Effects on Motor Activity and General CNS Function. A-740003 had no significant effect on motor coordination at doses up to 142 mg/kg i.p. [$F(3,31) = 0.35$, $p > 0.05$],

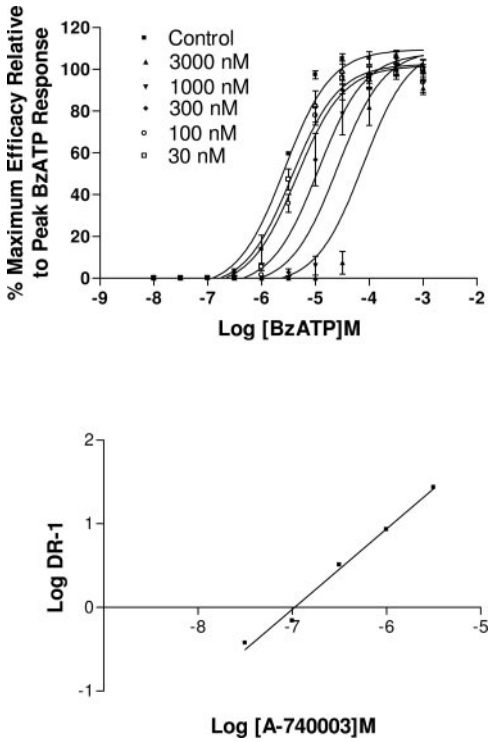

Fig. 6. A-740003 is a competitive antagonist at the $P2X_7$ receptor. Top, concentration-effect curves for BzATP-induced increases intracellular calcium concentrations were generated in the presence of increasing concentrations of A-740003. Curves are plotted as percent relative to the maximal response in the absence of A-740003. Bottom, Schild plot analysis of the antagonism produced by A-740003 with a slope = 0.98 ± 0.16 and a pA_2 of 7.0.

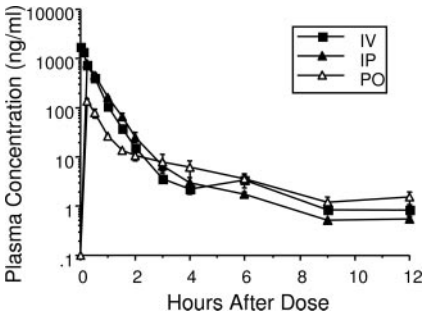

Fig. 7. Pharmacokinetic profile of A-740003 (5 μmol/kg i.v., i.p., and p.o.) in rats. The pharmacokinetic profile of A-740003 in rats was characterized by a high plasma clearance (3.7 l/h/kg), moderate oral bioavailability (F = 20%), a high volume of distribution (V_β = 21 l/kg), and a long plasma elimination half-life ($t_{1/2}$ = 4.0 h i.v.). C_{max} and T_{max} following oral administration at 2 mg/kg were 0.13 μg/ml and 2.5 h, respectively. In addition, A-740003 had good bioavailability (F = 79%) following i.p. administration at 2.3 mg/kg with a C_{max} of 0.76 μg/ml and a T_{max} of 0.25 h.

as measured by the ability of rats to run on an accelerating rotating rod (latency to fall for the control group, 58.1 ± 1.0 s; for the highest dose group, 56.3 ± 3.1 s). Rats were fully awake, responsive to stimuli, and retained the righting reflex, consistent with their ability to perform the Rotorod test at all of the doses tested.

Discussion

The present data demonstrate that A-740003 is a potent antagonist of rat and human $P2X_7$ receptors. A-740003

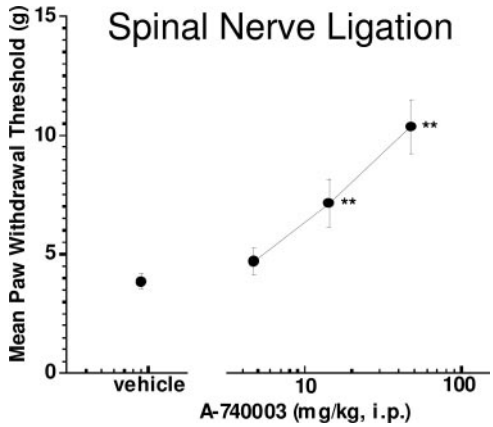

Fig. 8. Antinociceptive effects of A-740003 in the spinal nerve ligation model of neuropathic pain. Two weeks following L5-L6 spinal nerve injury, A-740003 was injected i.p. 30 min before testing. A-740003 demonstrated significant antiallodynic effects in neuropathic pain [$F(5,152)$ = 109.42, $p < 0.0001$]. Data represent mean ± S.E.M. **, $p <$ 0.01 as compared with vehicle-treated animals (n = 6–12 per group).

blocked $P2X_7$ receptor-mediated changes in intracellular calcium concentrations in a competitive fashion and was highly selective as compared with its activity at other P2 receptors as well as other cell surface receptors and ion channels. A-740003 also potently blocked other consequences of $P2X_7$ receptor activation including BzATP-evoked IL-1β release in differentiated human THP-1 cells and prolonged agonist-stimulated pore formation.

The discovery of A-740003 represents a significant advance in P2X receptor pharmacology since this compound is both more potent and more selective than other previously described $P2X_7$ receptor antagonists (Romagnoli et al., 2004). A-740003 also shows much less species differences in its ability to block both rat and human $P2X_7$ receptors as compared with the rat selective antagonist BBG and the human selective antagonist KN-62 (Anderson and Nedergaard, 2006). It is interesting to note that both of the latter antagonists are more than 10-fold more potent to block $P2X_7$ receptor-mediated pore formation (Yo-Pro uptake) as compared with their ability to block receptor-mediated calcium influx. The differential potency of these antagonists to block these $P2X_7$ receptor-mediated effects has been attributed to their relatively slow association kinetics in the two different assays (Namovic et al., 2005). In contrast, A-740003 showed equivalent potency to block both human $P2X_7$ receptor-mediated changes in intracellular calcium concentrations and Yo-Pro uptake. Similarly, an analysis of a series of novel phenyltetrazole-based $P2X_7$ antagonists (Nelson et al., 2006) indicates that antagonism of $P2X_7$ receptor-mediated changes in intracellular calcium concentrations, IL-1β release, and Yo-Pro uptake are positively correlated.

The activation of $P2X_7$ receptors results in the rapid maturation and extracellular release of the proinflammatory cytokine, IL-1β (Perregaux and Gabel, 1994; Solle et al., 2001; Ferrari et al., 2006). Other biochemical consequences of increased IL-1β concentrations include induction of nitric oxide synthase as well as increased production of cyclooxygenase-2 and tumor necrosis factor (TNF)-α (Woolf et al., 1997; Samad et al., 2001; Parvathenani et al., 2003). All of these proinflammatory events can also contribute to enhanced pain sen-

TABLE 3
Analgesic profile of A-740003 (i.p.)

Pain Model	ED_{50}	% Effect at 142 mg/kg i.p.
	mg/kg i.p.	%
Acute nociception		
Rat acute thermal	>142	0 ± 1
Inflammatory pain		
Carrageenan		
Acute thermal hyperalgesia	54	75 ± 5*
Edema	>142	36 ± 7*
(Complete Freund's adjuvant)		
Chronic thermal hyperalgesia	38	59 ± 16*
Edema	>142	0 ± 5
Neuropathic pain		
L5/L6 nerve ligation	19	65 ± 11* (47mg/kg)
Chronic constriction injury	114	55 ± 14*
Chemotherapy	142	51 ± 6*

* Significantly different ($p < 0.05$) from vehicle-treated animals (n = 6–12 per group).

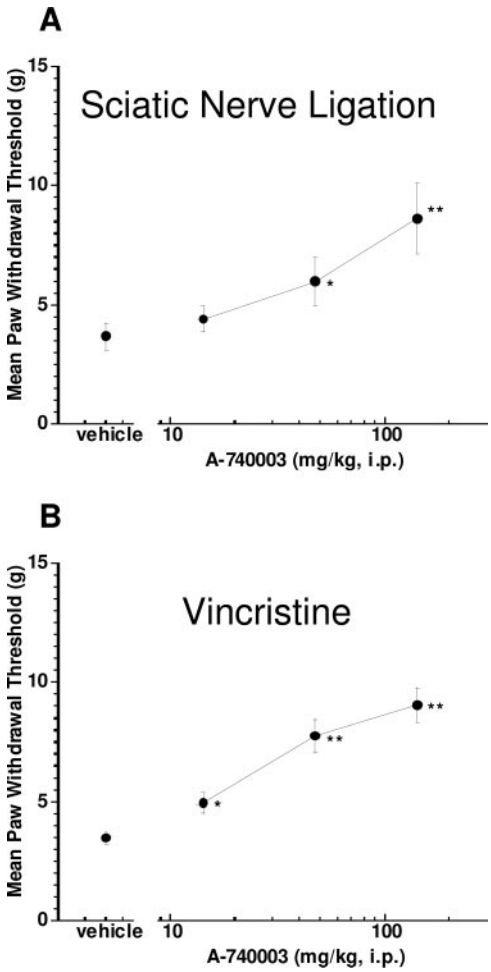

Fig. 9. Antinociceptive effects of A-740003 in CCI sciatic nerve injury- and vincristine-induced neuropathic pain. Two weeks following sciatic nerve injury (A) or continuous vincristine infusion (B), A-740003 was injected i.p. 30 min before testing. A-740003 demonstrated significant antiallodynic effects in both neuropathic pain models [A, $F(5,125) = 104.19$, $p < 0.0001$; B, $F(5,71) = 481.13$, $p < 0.0001$]. Data represent mean ± S.E.M. *, $p < 0.05$; **, $p < 0.01$ as compared with vehicle-treated animals (n = 6–12 per group).

sitivity (Woolf et al., 1997; Burnstock, 2006). The physiological significance of $P2X_7$ receptor modulation of IL-β release is evidenced by the reduced inflammatory phenotype of $P2X_7$ knockout mice (Solle et al., 2001; Labasi et al., 2002). ATP stimulation of macrophages from $P2X_7$ knockout mice does not result in the release of mature IL-1β, and $P2X_7$ knockout mice show significantly diminished inflammation in an experimental passive collagen-induced arthritis model (Labasi et al., 2002). A more recent study has demonstrated that $P2X_7$ knockout mice show reduced pain sensitivity following both complete Freund's adjuvant-induced inflammation and partial injury of the sciatic nerve (Chessell et al., 2005).

Similar to the nociceptive phenotype of mice lacking $P2X_7$ receptors (Chessell et al., 2005) or lacking both isoforms of IL-1 (Honore et al., 2006), systemic administration of A-740003 produced dose-dependent antinociceptive effects in models of neuropathic pain and inflammatory pain. A-740003 was particularly potent at reducing mechanical allodynia observed 2 weeks following L_5/L_6 nerve ligation. The antinociceptive activity of A-740003 in this model of neuropathic pain is consistent with recent reports of the analgesic efficacy of two other structurally distinct $P2X_7$ antagonists (Lappin et al., 2005; Nelson et al., 2006). A-740003 also significantly attenuated mechanical allodynia in two additional models of neuropathic pain: chronic constriction injury of the sciatic nerve and vincristine-induced neuropathic pain. The exact reasons for the differential potency of A-740003 to reduce tactile allodynia in these neuropathic pain models are unknown. However, these data may illustrate the preferential role of $P2X_7$ receptor modulation of IL-1β in reducing nociception in the SNL model as compared with the robust analgesic efficacy of a $P2X_3$ antagonist to reduce neuropathic allodynia in the chronic constriction injury of the sciatic nerve model (Jarvis et al., 2002).

A-740003 also significantly reduced thermal hyperalgesia in two models of inflammatory pain: intraplantar administration of complete Freund's adjuvant or carrageenan. The robust antinociceptive effects of A-740003 in these inflammatory pain models does not appear to be secondary to an anti-inflammatory effect since A-740003 was more efficacious at reducing nociception compared with paw edema in both of these models. It should be noted, however, that the anti-inflammatory activity of $P2X_7$ antagonists may be more pronounced in arthritis models as compared with acute (carrageenan) and subacute (CFA) inflammatory models where the contribution of IL-1β to ongoing inflammatory processes may be more prominent in chronic arthritis (Labasi et al., 2002).

Collectively, the present data and the phenotype of the $P2X_7$ knockout mice indicate a specific role for $P2X_7$ receptor activation in chronic pain states. It should be noted that Dell'Antonio et al. (2002a,b) have reported that local administration of oxidized-ATP, a weak and irreversible antagonist of $P2X_7$ receptors (Surprenant et al., 1996), reduced inflammation-induced mechanical hyperalgesia in rats. Although these investigators attributed these results to blockade of $P2X_7$ receptors, it must be appreciated that oxidized-ATP has weak affinity for $P2X_7$ receptors and also has many other pharmacological actions including blockade of $P2X_1$ and $P2X_2$ receptors (Evans et al., 1995) and inhibition of nuclear factor-κB and cytokine release (Murgia et al., 1993; Beigi et

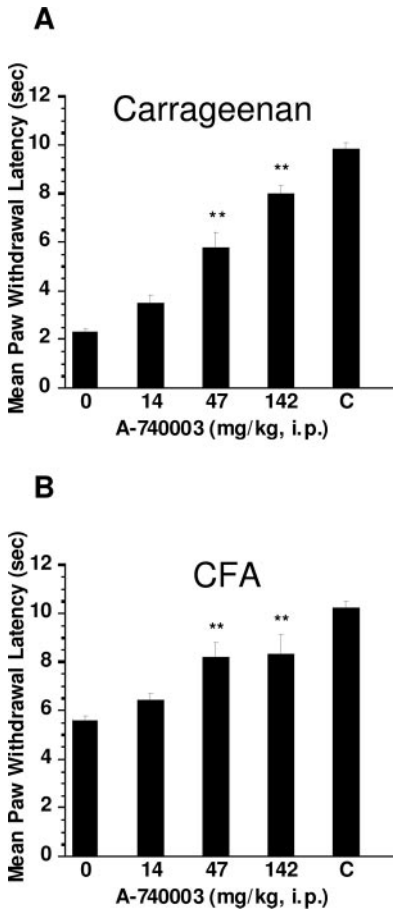

Fig. 10. Antinociceptive effects of A-740003 in inflammatory pain models. Two hours following carrageenan injection (A) or 2 days following CFA injection (B), A-740003 was injected i.p. 30 min before testing. A-740003 demonstrated significant antihyperalgesic effects in both models [A, $F(7,95) = 89.71$, $p < 0.0001$; B, $F(7,83) = 23.06$, $p < 0.0001$]. Data presented as bar graphs represent mean ± S.E.M. for the vehicle group (0 mg/kg i.p.), the three dose groups (14, 47, 142 mg/kg i.p.), and the contralateral side (C). **, $p < 0.01$ as compared with vehicle-treated animals ($n = 6$–12 per group). The doses were chosen as part of a testing strategy for project compounds to be compared with each other in micromoles per kilogram doses.

al., 2003; Di Virgilio, 2006). Consequently, the use of oxidized-ATP to block nociceptive responses in vivo cannot be taken as evidence for a specific role of $P2X_7$ in nociceptive signaling (Chessell et al., 2005; Anderson and Nedergaard, 2006).

The antinociceptive effects of A-740003 in chronic pain states are consistent with the mechanistic role of $P2X_7$ receptors in modulating IL-1β release and the ability of this pronociceptive cytokine to alter pain sensitivity in animal models. In addition to its proinflammatory effects, endogenous IL-1 levels are increased in the CNS in response to trauma associated with mechanical damage, ischemia, seizures, and hyperexcitability (Touzani et al., 2002). Increased IL-1 concentrations in the CNS also result in dose-dependent modulation of nociceptive signaling (Bianchi et al., 1998; Horai et al., 2000). At the level of the spinal cord, blockade of IL-1 receptors with the IL-1 receptor antagonist (IL-1ra) results in reduced nociception in animal models of inflammation and nerve-injury induced pain (Maier et al., 1993; Safieh-Garabedian et al., 1995; Sommer et al., 1999). These findings are further supported by the demonstration that exogenously applied IL-1 produces hyperalgesia when applied peripherally (Ferreira et al., 1988). In addition to the analgesic effects of the IL-1ra in experimental pain models, several genetic approaches have been used to further investigate the pronociceptive actions of IL-1 in mice. These include targeted gene disruption of the IL-1 type I receptor or the IL-1*acp*, as well as transgenic overexpression of the IL-1ra (Wolf et al., 2004) or IL-1$\alpha\beta$ double knockout (Honore et al., 2006). All of these approaches have produced mice that show reduced nociceptive responses relative to wild-type animals. Collectively, these data clearly indicate that $P2X_7$ receptor modulation of IL-1 contributes to nociceptive sensitivity in chronic pain states.

The present data further illustrate the multitude of mechanisms by which ATP can alter nociceptive sensitivity following tissue injury (Burnstock and Wood, 1996). Evidence from a variety of experimental strategies including genetic disruption and the development of selective antagonists has indicated that activation of several P2X receptors, including $P2X_3$, $P2X_{2/3}$, $P2X_4$ and $P2X_7$, and P2Y (e.g., $P2Y_2$) receptors, can modulate pain. For example, A-317491, a selective $P2X_3$ antagonist (Jarvis et al., 2002), effectively blocks both CFA-induced inflammatory thermal hyperalgesia as well as mechanical and thermal hyperalgesia resulting from chronic constriction of the sciatic nerve. Intrathecally delivered antisense oligonucleotides specifically targeting $P2X_4$ receptors have been shown to decrease tactile allodynia following nerve injury (Tsuda et al., 2003). In addition, activation of $P2Y_2$ receptors leads to sensitization of TRPV1 receptors (Tominaga et al., 2001; Lakshmi and Joshi, 2005). Thus, ATP acting at multiple purinergic receptors either directly on neurons (e.g., $P2X_3$, $P2X_{2/3}$, and P2Y receptors) or through indirect neural-glial cell interactions ($P2X_4$ and $P2X_7$) can alter nociceptive sensitivity (Tsuda et al., 2003; Zhang et al., 2005).

Taken together, the present data demonstrate that the acute in vivo blockade of $P2X_7$ receptors significantly reduces nociception in animal models of persistent neuropathic and inflammatory pain. Although there is growing appreciation for the role of $P2X_7$ modulation of proinflammatory IL-1 processing (Ferrari et al., 2006), the analgesic activity of A-740003 and other recently described selective $P2X_7$ receptor antagonists (Nelson et al., 2006) suggests a specific role for $P2X_7$ in neural-glial cells interactions associated with ongoing pain (Zhang et al., 2005).

References

Anderson CM and Nedergaard M (2006) Emerging challenges of assigning P2X (7) receptor function and immunoreactivity in neurons. *Trends Neurosci* **29:**257–262.

Armstrong JN, Brust TB, Lewis RG, and MacViar BA (2002) Activation of presynaptic P2X7-like receptors depresses mossy fiber-CA3 synaptic transmission through p38 mitogen-activated protein kinase. *J Neurosci* **22:**5938–5945.

Baraldi PG, del Carmen Nunez M, Morelli A, Flazoni S, Di Virglio F, and Romagnoli R (2003) Synthesis and biological activity of *N*-arylpiperazine-modified analogues of KN-62, a potent antagonist of the purinergic $P2X_7$ receptor. *J Med Chem* **45:**1318–1329.

Beigi RD, Kertesy SB, Aquilina G, and Dubyak GR (2003) Oxidized ATP (oATP) attenuates proinflammatory signaling via P2 receptor-independent mechanisms. *Br J Pharmacol* **140:**507–519.

Bennett GJ and Xie YK (1988) A peripheral mononeuropathy in rat that produces disorders of pain sensation like those seen in man. *Pain* **33:**87–107.

Bianchi BR, Lynch KJ, Touma E, Niforatos W, Burgard EC, Alexander KM, Park HS, Yu H, Metzger R, Kowaluk E, et al. (1999) Pharmacological characterization of recombinant human and rat P2X receptor subtypes. *Eur J Pharmacol* **376:**127–138.

Bianchi M, Dib B, and Panerai AE (1998) Interleukin-1 and nociception in the rat. *J Neurosci Res* **53:**645–650.

Burnstock G (2006) Pathophysiology and therapeutic potential of purinergic signaling. *Pharmacol Rev* **58:**58–78.
Burnstock G and Wood JN (1996) Purinergic receptors: their role in nociception and primary afferent neurotransmission. *Curr Opin Neurobiol* **6:**526–532.
Chakfe Y, Seguin R, Antel JP, Morissette C, Malo D, Henderson D, and Seguela P (2002) ADP and AMP induce interleukin-1 beta release from microglia cells through activation of ATP-primed $P2X_7$ receptor channels, *J Neurosci* **22:**3061–3069.
Chessell IP, Hatcher J, Bountra C, Michel AD, Hughes JP, Green P, Egerton J, Murfin M, Richardson J, Peck WL, et al. (2005) Disruption of the $P2X_7$ purinoceptor gene abolishes chronic inflammatory and neuropathic pain. *Pain* **114:**386–396.
Collo G, Neidhart S, Kawashima E, Kosco-Vibois M, North RA, and Buell G (1997) Tissue distribution of the $P2X_7$ receptor. *Neuropharmacology* **36:**1277–1283.
Dell'Antonio A, Quattrini A, Dal Cin E, Fulgenzi A, and Ferrero ME (2002a) Antinociceptive effect of a new P2Z/$P2X_7$ antagonist, oxidized ATP, in arthritic rats. *Neurosci Lett* **327:**87–90.
Dell'Antonio A, Quattrini A, Dal Cin E, Fulgenzi A, and Ferrero ME (2002b) Relief of inflammatory pain in rats by local use of the selective $P2X_7$ ATP receptor inhibitor, oxidized ATP. *Arthritis Rheum* **46:**3378–3385.
Di Virgilio F (2006) Novel data point to a broader mechanism of action of oxidized ATP: the $P2X_7$ receptor is not the only target. *Br J Pharmacol* **140:**441–443.
Donnelly-Roberts DL, Namovic M, Faltynek CR, and Jarvis MF (2004) Mitogen-activated protein kinase and caspase signaling pathways are required for $P2X_7$ receptor ($P2X_7R$)-induced pore formation in human THP-1 cells. *J Pharmacol Exp Ther* **308:**1053–1061.
Evans RJ, Lewis C, Buell G, Vlaera S, North RA, and Surprenant A (1995) Pharmacological characterization of heterologously expressed ATP-gated cation channels (P2X purinoceptors). *Mol Pharmacol* **48:**178–183.
Ferrari D, Pizzirani C, Adinolfi E, Lemoli RM, Curti A, Idzko M, Panther E, and DiVirgilio F (2006) The $P2X_7$ receptor: a key player in IL-1 processing and release. *J Immunol* **176:**3877–3883.
Ferreira S, Lorenzetti B, Bristow A, and Poole S (1988) Interleukin-1β as a potent hyperalgesic agent antagonized by a tripeptide analogue. *Nature (Lond)* **334:**698–700.
Honore P, Wade CL, Zhong C, Harris RR, Wu C, Ghayur T, Iwakura Y, Decker MW, Faltynek C, Sullivan J, et al. (2006). Interleukin-1$\alpha\beta$ gene-deficient mice show reduced nociceptive sensitivity in models of inflammatory and neuropathic pain but not post-operative pain *Behav Brain Res* **167:**355–364.
Horai R, Saijo S, Tanioka H, Nakae S, Sudo K, Okahara A, Ikuse T, Asano M, and Iwakura Y (2000) Development of chronic inflammatory arthropathy resembling rheumatoid arthritis in interleukin 1 receptor antagonist-deficient mice. *J Exp Med* **191:**313–320.
Humphrey BD and Dubyak GR (1996) Induction of the P2z/$P2X_7$ nucleotide receptor and associated phospholipase D activity by lipopolysaccharide and IFN-γ in the human THP-1 monocytic cell line. *J Immunol* **157:**5627–5637.
Jacobson KA, Jarvis MF, and Williams M (2002) Perspective: purine and pyrimidine: II. Receptors as drug targets. *J Med Chem* **45:**4057–4093.
Jarvis MF, Bianchi B, Uchic JT, Cartmell J, Lee C-H, Williams M, and Faltynek C (2004) [^{3}H]A-317491, a novel high-affinity non-nucleotide antagonist the specifically labels human $P2X_{2/3}$ and $P2X_3$ receptors. *J Pharmacol Exp Ther* **310:**407–416.
Jarvis MF, Burgard EC, McGaraughty S, Honore P, Lynch K, Brennan TJ, Subieta A, Van Biessen T, Cartmell J, Bianchi B, et al. (2002) A-317491, a novel potent and selective non-nucleotide antagonist of $P2X_3$ and $P2X_{2/3}$ receptors, reduces chronic inflammatory and neuropathic pain in rats. *Proc Natl Acad Sci USA* **99:**17179–17184.
Kahlenberg J and Dubyak GW (2004) Mechanisms of caspase-1 activation by $P2X_7$ receptor-mediated K^+ release. *Am J Cell Physiol* **286:**C1100–C1108.
Kim SH and Chung JM (1992) An experimental model for peripheral neuropathy produced by segmental spinal nerve ligation in the rat. *Pain* **50:**355–363.
Labasi JM, Petrushova N, Donovan C, McCurdy S, Lira P, Payette MM, Brissette W, Wicks JR, Audoly L, and Gabel CA (2002) Absence of the $P2X_7$ receptor alters leukocyte function and attenuates an inflammatory response. *J Immunol* **168:**6436–6445.
Lakshmi S and Joshi PG (2005) Co-activation of $P2Y_2$ receptor and TRPV channel by ATP: implications for ATP induced pain. *Cell Mol Neurobiol* **25:**819–32.
Lappin SC, Winyard LA, Clayton N, Chambers LJ, Demont EH, Chessell IP, Richardson JC, and Gunthorpe MJ (2005) Reversal of mechanical hyperalgesia in a rat model of inflammatory pain by a potent and selective P2X7 antagonist, in *Abstract 958.2 of the 35th Annual Society for Neuroscience Meeting*; 2005 Nov 12–16; Washington, DC. Society for Neuroscience, Washington, DC.
Lynch JJ 3rd, Wade CL, Mikusa JP, Decker MW, and Honore P (2005) ABT-594 (a nicotinic acetylcholine agonist): anti-allodynia in a rat chemotherapy-induced pain model. *Eur J Pharmacol* **509:**43–48.
Lynch KJ, Touma E, Niforatos W, Kage KL, Burgard EC, van Biessen T, Kowaluk EA, and Jarvis MF (1999) Molecular and functional characterization of human P2X(2) receptors. *Mol Pharmacol* **56:**1171–1181.
Maier SF, Wietelak EP, Martin D, and Watkins LR (1993) Interleukin-1 mediates the behavioral hyperalgesia produced by lithium chloride and endotoxin. *Brain Res* **623:**321–324.
Murgia M, Hanau S, Pizzo P, Rippa M, and Di Virgilio F (1993) Oxidized ATP: an irreversible inhibitor of the macrophage purinergic P2Z receptor. *J Biol Chem* **268:**8199–81203.
Namovic MT, Jarvis MF, and Donnelly-Roberts DL (2005) C-terminus P451L mutation does not alter the function of mouse recombinant $P2X_7$ receptors: a pharmacological comparison of mouse, rat and human $P2X_7$ receptors, in *Abstract 958.4 of the 35th Annual Society for Neuroscience Meeting*; 2005 Nov 12–16; Washington, DC. Society for Neuroscience, Washington, DC.
Nelson DW, Gregg RJ, Kort ME, Perez-Medrano A, Voight EA, Wang Y, Namovic MT, Grayson G, Donnelly-Roberts DL, Niforatos W, et al. (2006) Structure-activity relationship studies on a series of novel, substituted 1-benzyl-5-phenyltetrazole $P2X_7$ antagonists. *J Med Chem* **49:**3659–3666.
North AR (2002) Molecular Physiology of P2X Receptors. *Physiol Rev* **82:**1013–1067.
Panenka W, Jijon H, Herx LM, Armstrong N, Feighan D, Wei T, Yong VW, Ranshoff RM, and Macvicar BA (2001) $P2X_7$-like receptor activation in astrocytes increases chemokine monocyte chemoattractant protein-1 expression via mitogen-activated protein kinase. *J Neurosci* **21:**7135–7142.
Pannicke T, Fisher W, Biefermann B, Schadlich H, Grosche J, Faude F, Wiedemann P, Allgaier C, Illes P, Burnstock G, et al. (2000) $P2X_7$-receptors activation in Mueller glial cells from the human retina. *J Neurosci* **20:**5965–5972.
Parvathenani LK, Svetlana T, Greco CR, Roberts SB, Robertson B, and Posmantur R (2003) $P2X_7$ mediates superoxide production in primary microglia and is up-regulated in a transgenic mouse model of Alzheimer's disease. *J Biol Chem* **278:**13309–13317.
Perregaux DG and Gabel CA (1994) Interleukin-1β maturation and release in response to ATP and nigericin. *J Biol Chem* **269:**15195–15203.
Romagnoli R, Baraldi PG, Pavani MG, Tabrizi MA, Moorman AR, Di Virgilio F, Cattabriga E, Pancaldi C, Gessi S, and Borea PA (2004) Synthesis, radiolabeling, and preliminary biological evaluation of [3*H*]-1-[(*S*)-*N*,*O*-bis-(isoquinolinesulfonyl)-*N*-methyl-tyrosyl]-4-(*o*-tolyl)-piperazine, a potent antagonist radioligand for the $P2X_7$ receptor. *Bioorg Med Chem Lett* **14:**5709–5712.
Safieh-Garabedian B, Poole S, Allchorne A, Winter J, and Woolf CJ (1995) Contribution of interleukin-1 to the inflammation-induced increase in nerve growth factor levels and inflammatory hyperalgesia. *Br J Pharmacol* **115:**1265–1275.
Samad TA, Moore KA, Sapirstein A, Billet S, Allchorne A, Poole S, Bonventre JV, and Woolf CJ (2001) Interleukin-1beta-mediated induction of Cox-2 in the CNS contributes to inflammatory pain hypersensitivity. *Nature (Lond)* **410:**471–75.
Sim JA, Young MT, Sung HY, North RA, and Surprenant A (2004) Reanalysis of $P2X_7$ receptor expression in rodent brain. *J Neurosci* **24:**6307–6314.
Solle M, Labasi J, Perregaux DG, Stam E, Petrushova N, Koller BH, Griffiths RJ, and Gabel CA (2001) Altered cytokine production in mice lacking $P2X_7$ receptors. *J Biol Chem* **276:**125–132.
Sommer C, Petrausch S, Lindenlaub T, and Toyka K (1999) Neutralizing antibodies to interleukin1-receptor reduce pain-associated behavior in mice with experimental neuropathy. *Neurosci Lett* **270:**25–28.
Surprenant A, Rassendren F, Kawashima E, North RA, and Buell G (1996) The cytolytic P2z receptor for extracellular ATP identified as a P2X receptor (P2X7). *Science (Wash DC)* **272:**735–738.
Tominaga M, Wada M, and Masu M (2001) Potentiation of capsaicin receptor activity by metabotropic ATP receptors as a possible mechanism for ATP-evoked pain and hyperalgesia. *Proc Natl Acad Sci USA* **98:**6951–6956.
Touzani O, Boutin H, LeFeurve R, Parker L, Miller A, Luheshi G, and Rothwell N (2002) Interleukin-1 influences ischemic brain damage in the mouse independently of the interleukin-1 type 1 receptor. *J Neurosci* **22:**38–43.
Tsuda M, Shigemoto-Mogami Y, Koizumi S, Mizokoshi A, Kohsaka S, Salter M, and Inoue K (2003) $P2X_4$ receptors induced in spinal microglia gate tactile allodynia after nerve injury. *Nature (Lond)* **424:**778–783.
Verhoef PA, Estacion M, Schilling W, and Dubyak GR (2003) P2X7 Receptor-dependent blebbing and the activation of Rho-effector kinases, caspases, and IL-1 release. *J Immunol* **170:**5728–5738.
Wolf G, Yirmiya R, Goshen I, Iverfeldt K, Holmlund L, Takeda K, and Shavit Y (2004) Impairment of interleukin-1 (IL-1) signaling reduces basal pain sensitivity in mice: genetic, pharmacological and developmental aspects. *Pain* **104:**471–480.
Woolf CJ, Allchorne A, Safieh-Garabedian B, and Poole S (1997) Cytokines, nerve growth factor and inflammatory hyperalgesia: the contribution of tumour necrosis factor alpha. *Br J Pharmacol* **121:**417–424.
Zhang X-F, Han P, Faltynek CR, Jarvis MF, and Shieh C-C (2005) Functional expression of $P2X_7$ receptors in non-neuronal cells of rat dorsal root ganglion. *Brain Res* **1052:**63–70.

Address correspondence to: Dr. Michael F. Jarvis, Abbott Laboratories, R4PM, AP9A/311, 100 Abbott Park Road, Abbott Park, IL 60064. E-mail: michael.jarvis@abbott.com